Impact of Polyurethane Elasticity on the Gap between Polishing Tool and Work Surface in Elastic Emission Machining Systems

Ze Liu[1], Zebin Xia[1], Jiyu Pan[1], Peng Lyu[1], and Fengzhou Fang[1,#]

1 State Key Laboratory of Precision Measuring Technology & Instruments, Laboratory of Micro/Nano Manufacturing Technology, Tianjin University, Tianjin, 300072, China
Corresponding Author / Email: fzfang@tju.edu.cn

KEYWORDS: Elastic emission machining, Polishing gap, Roughness evolution, ACSM

Elastic emission machining (EEM) is an atomic-scale polishing method. It achieves atomic-scale material removal through the chemical adsorption of nanoparticles onto the workpiece surface, resulting in an ultra-smooth finish. As a non-contact processing method, the gap between the polishing tool and the workpiece surface significantly influences the machining effect. Since soft polyurethane materials are typically used for the polishing wheels, the elastic deformation of the material during machining affects the control of the polishing gap. In this study, an EEM setup is established, and the expansion of the polishing tool at different rotational speeds is calibrated using a laser displacement sensor. Additionally, a surface roughness evolution model is established. Through elastic emission machining of monocrystalline silicon, a surface roughness of 0.13 nm in Rq is achieved. This work provides technical support for the design and process optimization of EEM systems.

NOMENCLATURE

h_0 = initial gap
h = the gap distance between the work plane and the cylindrical surface of the wheel
R = polishing wheel radius
u_a = surface velocity
p = fluid pressure
μ = fluid viscosity
ΔR = the increase in radius
ρ = density of the polyurethane wheel
ω = angular velocity
E = Young's modulus of the polyurethane wheel

1. Introduction

The rapid advancement in modern optics has led to increasingly stringent requirements for optical components. These demands not only encompass exceptionally high surface figure accuracy and extremely low surface roughness but also necessitate virtually defect-free surfaces with impeccable quality[1,2]. For example, the Kirkpatrick-Baez mirrors in the European X-Ray Free Electron Laser require a shape error below 2 nm Peak-to-Valley (PV), while optical components in Extreme Ultraviolet Lithography demand a High-Spatial-Frequency Roughness under 100 pm Root Mean Square[3,4]. In the field of advanced light sources (ALS), microscopic surface defects in laser crystals used in high-power laser systems significantly impact the crystal's operational lifespan and damage threshold. To achieve elevated damage thresholds and extended operational longevity, the absence of surface lattice defects is required for laser crystal surfaces[5].

Conventional contact-based machining methods, which primarily rely on plastic deformation and brittle fracture mechanisms, are prone to inducing surface and subsurface damage such as microcracks and dislocations. Consequently, achieving atomic-level surface precision through these traditional approaches presents significant challenges due to the degradation of surface integrity[6,7]. Therefore, there is a critical need to develop a machining method capable of material removal at the atomic scale. Elastic emission machining (EEM), as a non-contact processing technique, offers exceptionally high machining precision. By leveraging chemical mechanisms, EEM can achieve atomic-scale material removal. This advanced methodology has found widespread application in the ultra-precision machining of various optical materials[8].

In 1980, Mori et al[9] proposed the EEM principle and developed the corresponding processing machinery. The polishing tool, immersed

in a polishing fluid, rotates at high speed while maintaining an extremely small gap from the workpiece surface. This configuration drives abrasive particles to impact the workpiece surface with the smallest possible incidence angle, realizing surface material removal at the atomic scale elastically. The gap between the polishing tool and the workpiece is a critical factor influencing the quality of the machining process. Mori et al.[10] proposed that the fluid in the EEM polishing zone exists in a laminar flow state, based on the Reynolds equation. Based on the Elasto-hydrodynamic Lubrication Theory, the relationship between the fluid film thickness distribution and pressure distribution in a two-dimensional space was established. For an idealized cylindrical polishing tool, Kim et al.[11] employed finite element method (FEM) to simulate the fluid motion in two-dimensional space and the forces acting on particles. In this study, the deformation of the polishing tool was neglected, and a model for material removal distribution was established. Kanaoka et al.[12] analyzed the relationship between fluid film thickness distribution and pressure distribution in three-dimensional space for a spherical polishing tool. Ma et al.[13] proposed a rolling model for the material removal mechanism in EEM, which considered the three-dimensional dynamic coupling relationship between fluid pressure and polishing wheel deformation. However, their study focused solely on the effect of fluid pressure on the polishing wheel, neglecting the deformation of the wheel itself due to rotation.

In this study, an EEM apparatus was constructed, and the deformation of the polishing tool was measured using a laser displacement sensor. Concurrently, modeling and simulation of the surface roughness evolution process were develpped.

2. Experimental setup

In this study, an apparatus for EEM was constructed. A cylindrical polishing wheel was employed in the setup. As illustrated in Fig 1, the apparatus primarily consists of a polishing wheel and a three-axis displacement stage. A detachable laser displacement sensor was employed to measure the deformation of the polishing wheel during rotation. The measurement accuracy of the sensor is 0.2 μm. During the machining process, a motor drives the rotation of the polishing wheel. The workpiece is fixed on the bottom displacement stage and immersed in the polishing fluid. The workpiece material is single-crystal silicon, and the polishing slurry contains 80 nm SiO_2 particles. The experimental parameters are listed in Table 1.

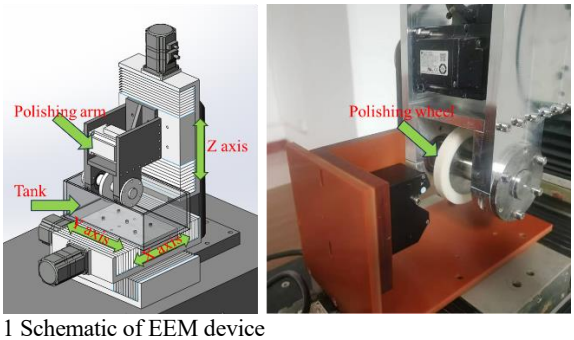

Fig. 1 Schematic of EEM device

Table 1 The experimental parameters

Parameter	Condition
Workpiece	Single-crystal silicon
Slurry	SiO_2
Particle diameter	80 nm
Rotation speed	1000 rpm
Initial gap	30 μm
Polishing time	1 h

3. Results and discussion

3.1 Deformation of the polishing wheel

During the EEM process, the workpiece and polishing wheel are immersed in a polishing fluid. Due to hydrodynamic effects, a fluid film forms between the rotating polishing wheel and the workpiece surface. In conventional EEM setups, the pressure applied to the polishing wheel and the hydrodynamic pressure of the fluid film achieve equilibrium, allowing automatic adjustment of the polishing wheel's position. However, in the present experimental apparatus, the gap between the polishing wheel and the workpiece is predetermined by the initial position of the displacement stage, and the polishing wheel's position remains fixed during the machining process. Fig. 2 shows a schematic diagram of EEM using the cylindrical polishing wheel. A cylindrical polishing wheel of radius R rotates with the surface velocity u_a at the minimum gap distance h_0 from the work surface.

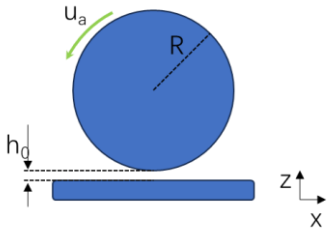

Fig. 2 Schematic diagram of EEM using the cylindrical polishing wheel.

The behavior of machining fluid between the rotating cylindrical surface and the flat plane can be described by the Reynolds equation.

$$\frac{d}{dx}\left(h^3\frac{dp}{dx}\right) = 6\mu u_a\frac{dh}{dx}$$

where p is the fluid pressure, μ is the fluid viscosity. The function h(x) is the gap distance between the work plane and the cylindrical surface of the wheel, and is obtained as following.

$$h(x) = h_0\left(1+\frac{x^2}{2Rh_0}\right)$$

The finite element method was employed to solve the above equations, yielding the fluid pressure distribution. This pressure was then transferred to the flexible polishing wheel through the fluid-solid interface, enabling the calculation of the polishing wheel's deformation under hydrodynamic pressure. The relationship between the maximum deformation of the polishing wheel and its rotational speed is illustrated

as Series 1 in Fig 3.

In this analysis, h_0 was set to 30 μm. It is noteworthy that the polishing wheel deformation obtained here only considers the effect of hydrodynamic pressure. However, the polyurethane polishing wheel, being an elastic body, undergoes expansion during rotation due to centrifugal forces. Based on the equilibrium between centrifugal force and stress, the relationship between the change in the polishing wheel's radius and its rotational speed can be expressed by the following equation:

$$\Delta R = \frac{\rho \omega^2 R^3}{E}$$

where ΔR is the increase in radius, ρ is the density of the polyurethane wheel, ω is the angular velocity, and E is the Young's modulus of the polyurethane wheel.

The experimental results obtained from the laser displacement sensor measurements are illustrated as Series 2 in Fig 3. The experimental results demonstrate that the deformation of the polishing wheel induced by rotational centrifugal force exceeds that caused by fluid dynamic pressure. Consequently, the deformation resulting from the rotation of the polishing wheel plays a significant role in controlling the polishing gap.

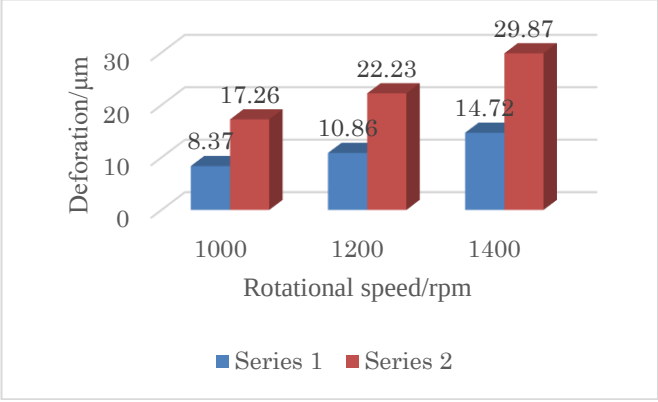

Fig. 3 The relationship between deformation of polyurethane wheels and rotational speed. Series 1 represents the deformation caused by fluid pressure, while Series 2 represents the deformation induced by centrifugal force.

3.2 Simulation of roughness evolution

Material removal in EEM depends on the chemical adsorption between polishing particles and the workpiece surface. Unlike traditional chemical etching, the relatively large size of the polishing particles in EEM results in selective interaction primarily with the irregularities of the topmost layer of the workpiece surface. The probability of abrasive particles entering microscopic pits is significantly lower. Hence, it is possible to achieve a high degree of surface planarization.

It is generally accepted that sharper peaks exhibit higher chemical reactivity, resulting in increased removal rates. Based on this principle, we developed a one-dimensional roughness model, postulating that the removal rate at each point is proportional to its local curvature. A numerical simulation was conducted to model the evolution of surface roughness with Rq 10 nm over time. The simulation results are presented in Fig 4.

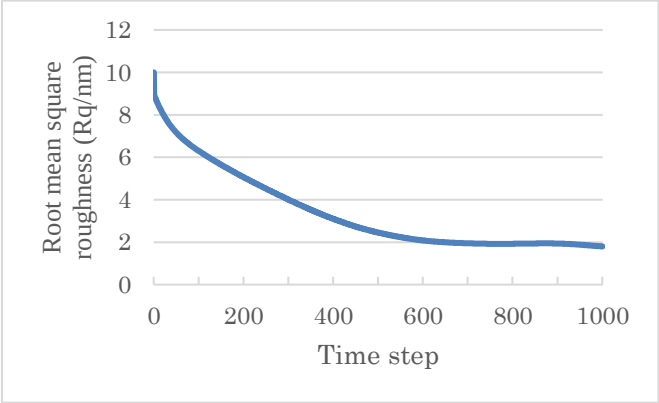

Fig. 4 Roughness evolution curve with time.

The computational simulation results substantiate the efficacy of EEM in reducing surface roughness. To corroborate these findings experimentally, the micromorphology of the silicon surface was examined using atomic force microscopy (AFM) before and after the polishing process, as illustrated in Fig 5(a) and 5(b), respectively. The root mean square (Rq) roughness of the silicon surface is improved from 0.48 nm to 0.13 nm, and an ultra-smooth surface is obtained.

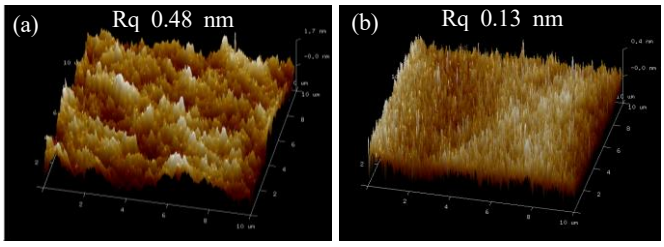

Fig. 5 Surface micromorphology before and after polishing.

4. Conclusions

In this study, an elastic emission machining apparatus was constructed, and a laser displacement sensor was utilized to measure the deformation of the polyurethane polishing wheel caused by centrifugal force. Comparing these measurements with the deformation induced by fluid dynamic pressure, as calculated using finite element methods, it was discovered that the deformation resulting from centrifugal force was twice that caused by fluid dynamic pressure. This finding demonstrates that centrifugal force-induced deformation is a crucial factor that cannot be neglected in controlling the polishing gap. Based on the material removal characteristics of elastic emission machining, numerical simulations were conducted to model the evolution of surface roughness, validating the capability of elastic emission machining to improve surface quality. Experimental results demonstrated the successful reduction of single-crystal silicon surface roughness from 0.48 nm in Rq to 0.13 nm in Rq.

ACKNOWLEDGEMENT

This work was supported by the National Natural Science Foundation of China (No. 52035009 and No. 52305498) and the

Postdoctoral Fellowship Program of CPSF (GZB20230512).

REFERENCES

1. Fang, F. Z., “On the Three Paradigms of Manufacturing Advancement,” Nanomanuf. Metrol., Vol. 6, No. 1, pp. 35, 2023.
2. Fang, F. Z., “The Three Paradigms of Manufacturing Advancement,” J. Manuf. Syst., Vol. 63, pp. 504–5, 2022.
3. Siewert, F., Buchheim, J., Gwalt, G., Bean, R. and Mancuso, A. P., “On the Characterization of a 1 m Long, Ultra-Precise KB-Focusing Mirror Pair for European XFEL by Means of Slope Measuring Deflectometry,” Rev. Sci. Instrum., Vol. 90, No. 2, pp. 021713, 2019.
4. Weiser, M., “Ion Beam Figuring for Lithography Optics,” Nucl. Instrum. Methods Phys. Res. B., Vol. 267, pp. 1390–93, 2009.
5. Stavros, G. S., Mike, S. and Mark, R. K, “Investigation of Processes Leading to Damage Growth in Optical Materials for Large-Aperture Lasers,” Appl. Opt., Vol. 41, No. 18, pp. 3628, 2002.
6. Mori, Y., Kazuya, Y., Katsuyoshi, E., Kazuto, Y., Kiyoshi, Y., Hidekazu, G., Hiroaki, K., Yasuhisa, S. and Hidekazu, M., “Creation of Perfect Surfaces,” J. Cryst. Growth., Vol. 275, No. 1–2, pp. 39–50, 2005.
7. Zhang, Y., Tang, J., Liang, S., Zhao, J., Hua, M., Zhang, C. and Deng, H, “Atomic-Scale Smoothing of Semiconducting Oxides via Plasma-Enabled Atomic-Scale Reconstruction,” Int. J. Mach. Tool. Manu., Vol. 196, pp. 104119, 2024.
8. Sidpara, A., “Elastic Emission Machining,” In Nanofinishing Science and Technology, CRC. Press, 2016.
9. Mori, Y., Kazuya, Y. and Katsuyoshi, E., “Elastic Emission Machining,” Precis. Eng., Vol. 9, No. 3, 1987.
10. Mori, Y., Okuda, T., Sugiyama, K. and Yamauchi, K., “Numerically controlled elastic emission machining - Consideration of machining property by motion analysis of powder particle in fluid.,” J. Jpn. Soc. Precis. Eng., Vol. 51, No. 5, pp. 1033–39, 1985.
11. Kim, J. D., “Motion Analysis of Powder Particles in EEM Using Cylindrical Polyurethane Wheel,” Int. J. Mach. Tools Manuf., Vol. 42, No. 1, pp. 21–28, 2002.
12. Kanaoka, M., Changling, L., Kazushi, N., Manabu, A., Hideo, Y., Yuzo, M., Hidekazu, M. and Kazuto, Y., “Processing Efficiency of Elastic Emission Machining for Low-thermal-expansion Material,” Surf. Interface Anal., Vol. 40, No. 6–7, pp. 1002–6, 2008.
13. Ma, W., Jiahui, L. and Xi, H., “Rolling Model Analysis of Material Removal in Elastic Emission Machining,” Int. J. Mech. Sci., Vol. 258, pp. 108572, 2023.